18th International Conference on
TRANSPORT AND SEDIMENTATION OF SOLID PARTICLES
11-15 September 2017, Prague, Czech Republic
ISSN 0867-7964 ISBN 978-83-7717-269-8

PARTICLE SETTLING USING THE IMMERSED BOUNDARY METHOD

Joep Goeree[1], Geert Keetels[1], Cees van Rhee[1]

[1] *Delft University of Technology, Dredging Engineering. Mekelweg 2, Delft, The Netherlands, Email:J.C.Goeree@tudelft.nl*

A vast range of processes involve hydraulic transport of particles, ranging from biological flows, environmental and hydraulic transport of raw materials from the seabed. Raw materials, found in the deep sea, are mined and transported from the deep sea to the surface. Typically this is done using a vertical hydraulic transport system or VTS. One of the challenges is to assure the flow, i.e. prevent possible clogging of the system. The particle sizes range from 1/10 to 1/3 of the VTS pipe diameter. The objective of this paper is to numerically simulate the settling of one particle at moderate particle Reynolds numbers (i.e. $Re_p \approx 100, 200$). Experimental data are used for validation. The equations of motion of a fluid flow are governed by the Navier-Stokes equations. These are discretized with the Finite Volume Method on a collocated grid and numerically solved using the fractional step method. Solids or particles are modeled using the Immersed Boundary Method (IBM).
In this paper a free settling particle in a confined domain, in two dimensions, is simulated. The particle size with respect to the domain size is varied in the calculation. The settling velocity is lower in comparison with a free settling particle in an infinite domain. This is due to the so-called wall effect. The settling velocity from the numerical calculation is compared with the corrected settling velocity known from experimental data. The computational and experimental results are qualitatively in agreement.

KEY WORDS: particle, IBM, deep sea, wall effect, CFD.

1. INTRODUCTION

In recent years deep sea mining attracted a considerable amount of attention. The presence of valuable raw materials in the deep sea is interesting, securing the supply of these materials in the long term. These materials can be found, typically at depths of 2000-5000 meters, in the form of manganese nodules, massive sulfides and cobalt rich crusts. The deposits contain several metallic materials such as manganese, iron, copper, nickel and cobalt. Furthermore, massive deposits also contain elements such as germanium, selenium, tellurium and indium, which are in high demand in many industries. These raw materials are transported hydraulically from the deep sea using a VTS. The flow assurance and stability of vertical hydraulic transport of particles was investigated experimentally by van

Wijk (2016).
In this work the Immersed Boundary Method is employed, introduced by Peskin (1972), describing a particle settling under gravity, with a diameter ranging from 1/10 to 1/3 with respect to the pipe diameter. The need for grid generation, which is numerically cumbersome in combination with moving bodies, is removed. This makes this method suitable in complex flows (as described above). The use of IBM is an active research field and gained considerable attention in the last decades, see for instance Peskin (2002), Fadlun et al. (2000), Ghosh and Stockie (2013) or Wang et al. (2017).

2. IMMERSED BOUNDARY METHOD

2.1. EQUATIONS OF MOTION

The motion of a fluid is described with the Navier-Stokes equations and is given by:

$$\frac{\partial \rho\, \mathbf{u}}{\partial t} + \nabla \cdot (\rho\, \mathbf{uu}) = -\nabla p + \nabla \cdot \left(\mu \left(\nabla \mathbf{u} + \nabla \mathbf{u}^T\right)\right) + \mathbf{s} \tag{1}$$

where u, ρ, μ, and p are the velocity, density, molecular viscosity and the hydrodynamic pressure, respectively. The source term, s, in Equation (1) is a body force, e.g. a buoyancy force due to density differences of a fluid. The incompressibility constraint, or conservation of mass, is expressed as:

$$\frac{\partial \rho}{\partial t} + \nabla \cdot (\rho\, \mathbf{u}) = 0 \tag{2}$$

The body force, s, see Equation (1), consists of two forces:

$$\mathbf{s} = \mathbf{f}_{IB} + \mathbf{f}_g \tag{3}$$

where f_g is the force due to the gravity acting on an immersed solid:

$$\mathbf{f}_g = (\rho_s - \rho_f)\, \mathbf{g} \tag{4}$$

here ρ_s is the density of the solid particle. The density difference causes the solid to settle under gravity. In Equation (3) the variable, f_{IB} , is the immersed body force. The immersed body force is imposed in Equation (1) in such a way that a desired or imposed velocity, denoted as V, is recovered. The numerical treatment of the immersed body force and the imposed velocity, V, will be discussed in more detail in section Section 3.

2.2. SOLIDS

The Immersed Boundary Method (IBM) was introduced by Peskin (1972) describing the interaction between a fluid and a solid, in this case valves in a human heart. A more elaborate discussion of the method is given by Fadlun et al. (2000) or Peskin (2002). Here this method is used modeling a solid particle, with a particular shape, settling in a fluid. A mask function, discussed in more detail in Section 3.2, is used denoting the solid region, see Figure 1. In this region the solid density, ρ_s , differs from the density of the surrounding fluid, ρ_f . Moreover, by setting the viscosity to a high value, in the solid region, the body is made non-deformable.

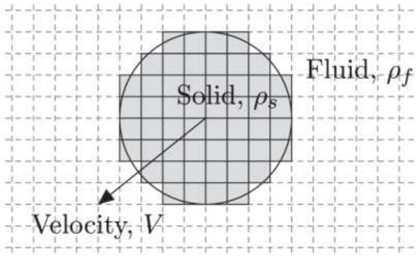

Figure 1: Schematic drawing of the Immersed Boundary Method.

2.3. WALL EFFECT

The terminal settling velocity, of a particle settling in a confined space, is lower, than the terminal settling velocity of a particle settling in an infinite domain. The reduced settling velocity is influenced by the presence of a wall and this phenomenon is called the wall effect. In the following the wall effect formulation, proposed by di Felice (1996) is briefly discussed. The wall effect can be quantified by defining a wall factor, f, as the velocity ratio:

$$f = \frac{V}{V_\infty} \tag{5}$$

where V is the falling velocity of a sphere settling in a tube, of a certain dimension, filled with a liquid. The terminal settling velocity, of the same sphere, in an unbounded domain is denoted by V_∞. The wall factor, f, is a function of the ratio of the particle size and the domain size, the diameter of the tube and the particle Reynolds number, Re_p, at terminal settling velocity V_∞, with $Re_p = \rho_f V_\infty d_p / \mu$. The following correlation, for the wall factor f Equation (5), based on experimental data reported by Fidleris and Whitmore (1961), has been introduced by di Felice (1996):

$$f = \left(\frac{1-\lambda}{1-0.33\lambda}\right)^{\alpha} \tag{6}$$

where the particle tube diameter ratio is $\lambda = d_p/D$. In Equation (6), α depends on Re_p at terminal settling velocity V_∞, see di Felice (1996), in the following manner:

$$\frac{3.3-\alpha}{\alpha-0.85} = 0.1Re_p \tag{7}$$

The relations, Equation (6) and Equation (7), are valid for the intermediate flow regime, i.e. $Re_p \leq 200$. The reduction of the terminal settling velocity due to the wall effect, introduced here, is used as comparison with computational results from the numerical model.

3 NUMERICAL MODELING

3.1 FRACTIONAL STEP METHOD

The Navier-Stokes equations, see Equation (1), are discretized using the Finite Volume Method, (FVM), Versteeg and Malalasekera (1995), Ferziger and Peric (1999). The motion of the flow is solved using the fractional step method, Chorin (1968). The high diffusion coefficient, μ , in the solid region, leads to numerical instabilities. A method circumventing numerical instabilities is to use an implicit fractional step method. Moreover, an extra body force is added, accounting for the influence of the immersed solid. The (implicit) fractional step algorithm is described in the following, given in semi-discretized from:

$$\frac{\rho \mathbf{u}^* - \rho \mathbf{u}^n}{\Delta t} = -\mathbf{A}(\mathbf{u}^n) + \mathbf{D}(\mathbf{u}^*) + \mathbf{f}_{IB} + \mathbf{f}_g \tag{8}$$

Where Δt is the time step size, $A(u^n)$ the advective term, $D(u^*)$ the viscous contribution and u^* is a first predictor of the velocity. Equation (8) needs to be solved implicitly with a matrix solver. In this work the BiCGStab algorithm, see Press et al. (1992), is chosen and is readily available in the C++ Eigen package, see Guennebaud et al. (2010). Note, that the gradient of the pressure is omitted in Equation (8). The pressure can be recovered with help of the continuity constraint and, Equation (2) and the predictor step, Equation (8). This results in the so-called pressure Poisson equation:

$$\nabla^2 p^{n+1} = \frac{1}{\Delta t}\left(\nabla \cdot (\rho \mathbf{u}^*) + \left(\frac{\partial \rho}{\partial t}\right)^n\right) \tag{9}$$

The pressure Poisson equation is solved using a multi grid solver, see Briggs et al. (2000) and Press et al. (1992). Finally the velocity, at the next time level, is obtained with the newly found pressure and the predictor velocity, Equation (9) and Equation (8):

$$\rho \mathbf{u}^{n+1} = \rho \mathbf{u}^* - \Delta t \nabla p^{n+1} \tag{10}$$

The immersed boundary force, f_{IB} , is yet to be determined. The IBM body force, to get the desired velocity, V^{n+1}, is given by:

$$\mathbf{f}_{IB} = \begin{cases} \left(\rho \mathbf{V}^{n+1} - \rho \mathbf{u}^n\right)/\Delta t = & \\ \mathbf{A}(\mathbf{u}^n) - \mathbf{D}(\mathbf{u}^n) - \mathbf{f}_g + \nabla p & \text{if} \quad \text{inside immersed solid} \\ 0 & \text{if} \quad \text{outside immersed solid} \end{cases} \tag{11}$$

3.2. MOTION OF IMMERSED SOLID

The motion of the immersed solid is governed by the density difference between the solids density and the surrounding fluid. The immersed solid is marked using a mask function, wherein the density and viscosity differ from the surrounding fluid. In the masked region the viscosity is set to a high value in order to make a non-deformable body. At each time step the solid region is transported using an advection equation, which is formulated as follows:

$$\frac{\partial \phi}{\partial t} + \nabla \cdot (\phi \mathbf{u}) = 0 \tag{12}$$

where ϕ is the transported mask function at which the solids region moves. Here ϕ is of binary form, with:

$$\phi = \begin{cases} 1 & \text{if} \quad \text{inside immersed solid} \\ 0 & \text{if} \quad \text{outside immersed solid} \end{cases} \tag{13}$$

The transported quantity, ϕ, needs to be positive at all times, i.e. the numerical solution needs to be bounded. This is achieved by employing the van Leer flux limiter, Van Leer (1974). Moreover, the numerical solution of the transport equation, Equation (12), suffers from numerical diffusion (as every numerical solution does). Therefore, at the each time step the particle shape is re-initialized. The re-initialization is done as follows. At each time step the center of gravity, (COG), and the (volume) averaged velocity, V^{n+1}, of the masked region is determined. The position of the COG is advanced in time, using a simple forward Euler step, with the average velocity of the COG. At the new location of the COG the particle shape is re-initialized with a new mask region. It should be noted that rotation of the particle is neglected.

3.3. TERMINAL SETTLING VELOCITY

The terminal settling velocity of a particle in a quiescent fluid in an infinite domain is described with Newton's second law. In steady state i.e. at terminal settling velocity, three forces govern the motion of a particle. The forces are the buoyancy, gravity and drag force. The buoyancy and gravity force can be formulated with the following single expression:

$$F_g = \frac{4\pi}{3} \left(d_p/2\right)^3 g_z \left(\rho_s - \rho_f\right) \tag{14}$$

where F_g is the difference between the gravity, the diameter of the particle is D and the variables ρ_s and ρ_f are the solids and fluid density respectively. Finally the variable g_z denotes the gravitational constant in, using a Cartesian coordinate system, z -direction. The drag force is formulated as follows:

$$F_d = \frac{1}{2} C_d \rho_f V_\infty^2 \pi \left(d_p/2\right)^2 \tag{15}$$

where V_∞ is the terminal velocity of a particle and C_d the drag coefficient. Combining Equation (14) and Equation (15) the terminal velocity yields:

$$V_\infty = \sqrt{\frac{4 g_z \, d_p \left(\rho_s - \rho_f\right)}{3 C_d \rho_f}} \tag{16}$$

it should be noted that the drag coefficient governs the settling velocity. Since in this work a 2D numerical calculation is shown, Equation (14) and Equation (15) needs to be adjusted accordingly. Basically in a 2D geometry cylinders are settling instead of spherical particle. This can be achieved by considering the a cylinder with a diameter d_c with a length l and take the length $l \rightarrow \infty$. Equation (14) can be rewritten into the following form, see Ghosh and Stockie (2013):

$$\overline{F}_g = \frac{\pi}{4} g_z l d_c^2 \left(\rho_s - \rho_f\right) \tag{17}$$

and the drag force becomes:

$$\overline{F}_d = \frac{1}{2} C_d \rho_f V_\infty d_c l \tag{18}$$

Wherein the $\overline{F}_d$ and $\overline{F}_g$ denote drag and gravity force, in a 2D geometry, respectively. By using Equation (17) and Equation (18) the terminal settling velocity of a cylinder can be obtained:

$$V_\infty = \sqrt{\frac{\pi g d_c \left(\rho_s - \rho_f\right)}{2 C_d \rho_f}} \tag{19}$$

Now the terminal settling velocity, which depends on the drag coefficient C_d, can be calculated. In turn the drag coefficient is a function of the particle Reynolds number, Re_p .

4. RESULTS

4.1. NUMERICAL SETUP

Two cases are considered here, in which the ratio of the particle diameter, d_p and the channel width, D, is varied. These ratios are respectively, $d_p/D \approx 1/10$ and $d_p/D \approx 1/3$. In the calculations the particle size, d_p , was kept constant and the width, D, of the channel was varied. At the walls no slip boundary conditions were imposed. The C_d value, in order to determine the terminal settling velocity, Equation (19), originates from Rajani et al. (2009) and Zdravkovich (1997) and is approximately $C_d \approx 1.33$ at a $Re_p \approx 200$. It should be noted that the densities of manganese nodules are in the range of 2000-2500 [kg/m^3], this deviates from the values chosen in the numerical benchmark.

Table 1

Physical properties, these are used as input in the calculation.

Particle diameter d_p $[m]$	particle density ρ_p $[kg/m^3]$	fluid density ρ_f $[kg/m^3]$	fluid viscosity μ $[Pas]$
0.09	1050	1000	0.1

Table 1 and Table 2 show the physical properties and numerical parameters used in the calculation. Figure 2 shows the particle trajectory, subplot (a) , and the particle velocity, subplot (b) .

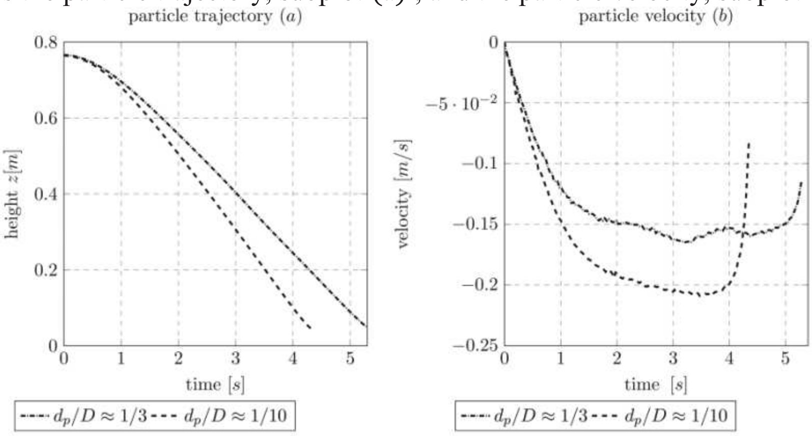

Fig 2. Particle trajectory, see (a) and particle velocity (b) shown here for ratio of $d_p/D \approx 1/10, 1/3$.

Table 2

Numerical parameters used in the calculation.

d_p/D ratio	Resolution $n_x \times n_z$	Height H $[m]$	Width D $[m]$	drag coeff. C_d $[-]$
1/3	53×159	0.9	0.3	1.33
1/10	159×159	0.9	0.9	1.33

4.2. COMPARISON WITH WALL CORRECTED VELOCITIES

Here the wall corrected velocities are compared here with the results of the calculations. The comparison is made using Equation (6) and Equation (7) and experimental data. Figure 3 shows the results from the two calculations, $d_p/D \approx 1/3, 1/10$, with the experimental data and the wall corrected fit function. The horizontal axis is the ratio between the particle diameter and the channel width, d_p/D . The vertical axis is the settling velocity scaled with the terminal settling velocity of a particle in an infinite domain, V/V_∞. It is assumed that the wall effect, Equation (6) and Equation (7), determined in a 3D geometry, i.e. a spherical particle settling in a tube, holds for a 2D geometry. The computational results, the two simulated cases, do not fully agree with the experimental data from Fidleris and Whitmore (1961) and the wall corrected fit function introduced by Felice (1996), Equation (6) and Equation (7). However, settling velocity for the $d_p/D \approx 1/3$ case is lower than the settling velocity of the $d_p/D \approx 1/10$ case. Moreover, it can be seen in Figure (3) that for the $d_p/D \approx 1/10$ case, the terminal settling velocity of the particle converges to the terminal settling velocity of a single particle, in stagnant fluid, in an infinite domain.

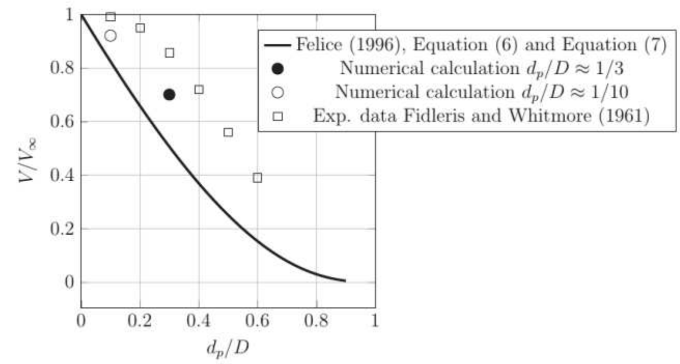

Fig. 3 Wall corrected settling velocity, experimental data, fit function and results from 2D calculation.

5. SUMMARY AND CONCLUSIONS

In this paper a numerical method is presented describing a single particle settling under gravity using the Immersed Boundary Method. The Navier-Stokes equations are solved using the fractional step method. The particle shape is marked using a masked function and transported with an advection equation. At every time step the particle shape is reinitialized around the center of gravity of the mask function.

From experiments it is known that the settling velocity is less for a particle in a confined space with respect to a particle settling in an infinite domain. This is known as the so-called wall effect. Here two 2D calculations, a particle settling under gravity in a confined space, have been performed as a validation of the numerical method.

The computational results have been compared with experimental data and empirical relations The two simulated cases, with a particle domain ratio of 1/10 and 1/3 respectively, agree qualitatively with the experimental results found in literature.

ACKNOWLEDGEMENTS

This research is supported by the Blue-Mining project, (www.bluemining.eu), and has received funding from the European Union's Seventh Framework Program for research, technological development and demonstration under Grant Agreement no. 604500. The authors are grateful for their support.

REFERENCES

Briggs, W. L., Van Emden, H., and McCormick, S. F. (2000). *A Multigrid Tutorial (2Nd Ed.)*. Society for Industrial and Applied Mathematics, Philadelphia, PA, USA.

Chorin, A. J. (1968). Numerical solution of the navier-stokes equations. *Mathematics of Computation*, 22(104):pp. 745–762.

Fadlun, E., Verzicco, R., Orlandi, P., and Mohd-Yusof, J. (2000). Combined immersed boundary finite difference methods for three dimensional complex flow simulations. *J. Comput. Phys.*, 161:35–60.

Felice, R. D. (1996). A relationship for the wall effect on the settling velocity of a sphere at any flow regime. *International Journal of Multiphase Flow*, 22(3):527 – 533.

Ferziger, J. H. and Peric, M. (1999). *Computational Methods for Fluid Dynamics*. Springer, New York, 2nd edition.

Fidleris, V. and Whitmore, R. L. (1961). Experimental determination of the wall effect for spheres falling axiall in cylindrical vessels. *British Journal of Applied Physics*, 12:490–494.

Ghosh, S. and Stockie, J. M. (2013). Numerical simulations of particle sedimentation using the immersed boundary method. *arXiv:1304.0804v2 [physics.flu-dyn]*.

Guennebaud, G., Jacob, B., et al. (2010). Eigen v3. http://eigen.tuxfamily.org.

Peskin, C. S. (1972). Flow patterns around heart valves: A numerical method. *Journal of Computational Physics*, 10(2):252 – 271.

Peskin, C. S. (2002). The immersed boundary method. *Acta Numerica*, 11:479–517.

Press, W. H., Teukolsky, S. A., Vetterling, W. T., and Flannery, B. P. (1992). *Numerical Recipes*. Cambridge University Press, Cambridge.

Rajani, B., Kandasamy, A., and Majumdar, S. (2009). Numerical simulation of laminar flow past a circular cylinder. *Applied Mathematical Modelling*.

Van Leer, B. (1974). Towards the ultimate conservative difference scheme ii. monotonicity and conservation combined in a second order scheme. *J. Comp. Phys.*, 14(4).

van Wijk, J., A.M.Talmon, van Rhee (2016). Stability of vertical hydraulic transport processes for deep ocean minin: An experimental study. *Ocean Engineering,* 12:203-213

Versteeg, H. K. and Malalasekera, W. (1995). *An Introduction to Computational Fluid Dynamics, The finite Volume Method.* Prentice Hall, London.

Wang, Y., Shu, C., Yang, L., and Teo, C. (2017). An immersed boundary-lattice boltzmann flux solver in a moving frame to study three-dimensional freely falling rigid bodies. *Journal of Fluids and Structures*, 68:444 – 465.

Zdravkovich, M. (1997). *Flow Around Circular Cylinders*. Oxford Science Publications.